JOURNAL OF CATALYSIS 48, 237–242 (1977)

Chemisorption and Catalysis on Oxidized Aluminum Metal

PAUL K. HANSMA[1]

Department of Physics, University of California, Santa Barbara, California 93106

AND

D. A. HICKSON AND J. A. SCHWARZ[2]

Chevron Research Corp., Richmond, California 94800

Received December 31, 1976

The oxide that grows on aluminum metal on exposure to room temperature air is similar in both its physical and chemical properties to γ-alumina. Thermal gravimetric analysis shows that it is not an aluminum hydrate. Vibrational spectroscopy of adsorbed pyridine shows that Lewis acid sites can be generated by fluoriding.

I. INTRODUCTION

Inelastic electron tunneling spectroscopy (IETS) (*1*, *2*) is the most sensitive technique known for vibrational spectroscopy: one monolayer over an area of 0.2×0.2 mm is a typical sample size. As little as 1/30 of a monolayer can be analyzed (*3*). This high sensitivity is especially valuable for vibrational spectroscopy of adsorbed surface species. Comparative studies have shown the sensitivity of tunneling spectroscopy to be superior to infrared and Raman spectroscopy on the same system (*4–6*).

Unfortunately, not all adsorbents can be studied by tunneling spectroscopy. In fact, almost all work to date has been on adsorbed species on aluminum that was oxidized in air or oxygen. Fortunately, aluminum oxide is interesting both as a catalyst itself and as a catalyst support. The question naturally arises: How is oxidized aluminum used in tunneling spectroscopy related to aluminum oxides used in conventional catalysts? A partial answer to this question can be found in the comparison studies mentioned above (*4–6*). In each case the adsorbed species on oxidized aluminum films detected by tunneling spectroscopy was the same as detected by optical techniques on γ-alumina.

The approach we have taken to answering the above question is to prepare an oxidized aluminum surface with large enough area to use conventional catalyst evaluation techniques. This can be done by making and then oxidizing small aluminum particles (*7*). We report the results of electron microscopy, thermal gravimetric analysis (TGA), and catalytic testing on such particles. Further, we report tunneling spectroscopic results on pyridine adsorption to determine the oxide acidity.

By conventional[3] catalyst evaluation

[1] Alfred P. Sloan Foundation Fellow (1975–1977). Work supported by National Science Foundation.

[2] Presently at Exxon Corp., P. O. Box 45, Linden, N.J. 07036.

[3] Conventional, except that the study of adsorbed pyridine was done by tunneling spectroscopy rather than infrared spectroscopy.

ISSN 0021-9517

techniques, we found that oxidized aluminum used for tunneling spectroscopy studies closely resembles commercial γ-alumina in both physical and chemical properties. We conclude that tunneling studies of adsorbed species, both on oxidized aluminum and on metals supported on oxidized aluminum (*8*), will be relevant in catalytic research.

II. PARTICLE PREPARATION

The particles were prepared by evaporating Al metal from a W filament in 10 Torr of argon and scraping the resultant particles from the walls of a 20 × 20 × 30 cm Al box that surrounded the filament. Approximately 10 evaporations were required to produce the 2 g of particles used in this research.

The particles were oxidized by exposure to room temperature air from the date of preparation to testing ($\approx$2 weeks). They formed only a thin, surface film of oxide verified by hydrogen evolution from a solution of sodium hydroxide (*9*). The particles are thus similar to the electrodes used in tunneling spectroscopy.

III. PHYSICAL CHARACTERIZATION

A. *Electron Microscopy*

Electron micrographs of the alumina sample were obtained by ultrasonically dispersing the sample in *n*-butyl alcohol and placing a microdroplet onto a 200 μm carbon-coated copper microscope grid. Micrographs at 10,000 and 25,000 diameters and selected area diffraction patterns were made using a JEOL-6A electron microscope. Figure 1 shows an electron micrograph of the Al particles. The spherical particles have an average radius of $\approx$800 Å. The theoretical surface area of such particles is $\approx$14 m^2/g.

B. *Surface Area Measurements*

Conventional N_2 BET surface area measurements were made on the oxidized Al particles. The surface area was 13.6 m^2/g, which agreed excellently with the theoretically calculated surface area.

Thermal analytical measurements were made on a DuPont 951 thermal gravimetric analyzer (TGA). Approximately 20–24 mg samples were loaded under ambient conditions onto the platinum pan of the microbalance and the furnace tube was sealed in place. Nitrogen was passed through the furnace and around the sample at a 100 ml/min flow rate. The nitrogen was dried over Drierite and had approximately 40 ppm of oxygen. The furnace temperature was increased at 10°C/min from room temperature to 550°C. Sample weight and differential weight losses as a function of temperature were recorded.

From room temperature to 200°C some mass loss occurred (0.7% of total mass, $\approx$3% of oxide mass). This is observed with all aluminas that have been exposed to air (*10*). It is due to loss of physically adsorbed water. From 200 to 400°C there was little, if any, mass loss (<0.01% of total mass, <0.05% of oxide mass). This suggests that the surface layer is Al_2O_3, not an aluminum hydroxide (*11*),[4] since dehydration of aluminum hydroxides occurs below 400°C (*12*). There is, however, a layer of surface hydroxyl groups always seen with tunneling spectroscopy. These *surface* hydroxyl groups will not all be removed until much higher temperature, >1000°C (*10*) though some will be removed at lower temperatures. This dehydroxylation has important consequences for the surface chemistry of alumina. Above 400°C there is a rapid mass increase, probably due to further oxidation of the particles.

IV. CHEMICAL CHARACTERIZATION

A. *Butene-1 Isomerization*

Butene-1 activities of the alumina particles were estimated by comparison with

[4] This conclusion was reached independently, from different data (11).

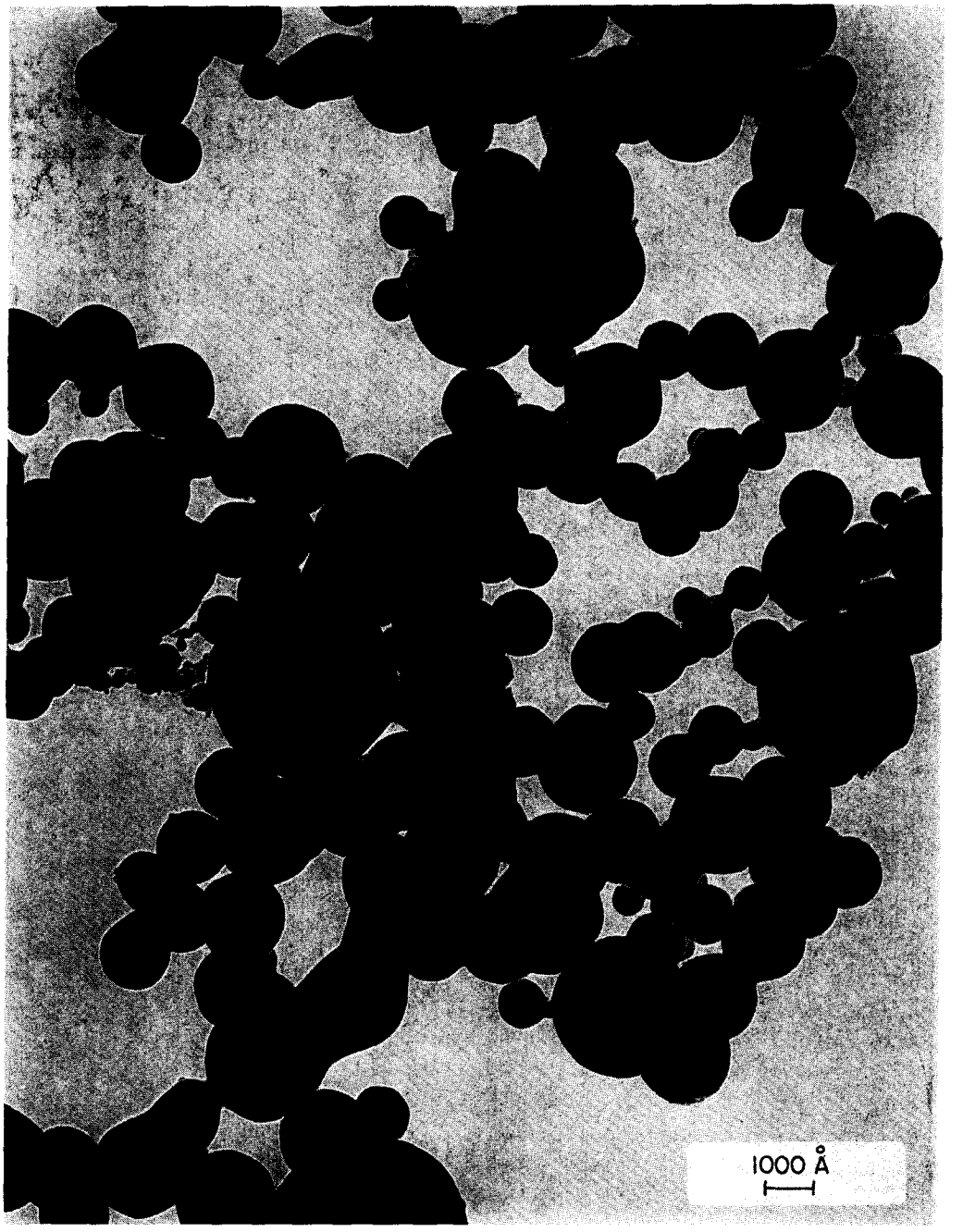

FIG. 1. Electron micrograph of small Al particles formed by the evaporation of Al metal in argon at a pressure of 10 Torr. The particles were oxidized in air and studied with standard catalyst evaluation techniques to characterize the oxide that grows on Al metal.

a standard γ-alumina (Harshaw alumina C-111923 calcined in air for 4 hr at 677°C). Approximately 1 ml of sample was charged to a glass reactor. The sample was treated 2 hr in flowing helium at 1 atm and 260°C, then cooled to the test temperature of 204°C. Feed consisting of 20% butene-1 in helium was passed through the catalyst at

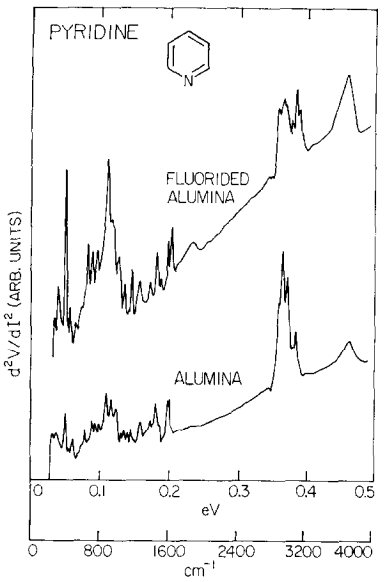

FIG. 2. Tunneling spectrum of pyridine vapor doped onto the oxide of Al–oxide–Pb junctions. For the upper trace the oxidized aluminum had been pretreated with a solution of ammonium fluoride in water spun on in the usual manner. Both the fluorided and unfluorided oxidized aluminum strips were returned to a high-vacuum system, baked for 60 sec with a quartz iodide lamp in high vacuum, and then exposed to 1 Torr of pyridine vapor for 90 sec. The junctions were completed with the usual evaporated lead electrodes.

9 cm^3/min (NTP), and the effluent stream was sampled after 75 min onstream exposure and analyzed by gas chromatography. Reaction mix product analyses were accomplished on a 22-ft 10% EDO-1 on 100–200 mesh firebrick at 0°C. Conversions were computed from the gas chromatographic analyses of reaction mix products. The experiment was then repeated using the standard alumina. The relative specific rate of reaction was expressed as follows:

$$\text{relative rate} = \frac{XW^0A^0}{X^0WA},$$

where X = the conversion at fixed catalyst volume, temperature, space rate, and sample time for the test; W = the sample weight (grams); A = the sample surface area (m^2/gram); the superscripts refer to the reference alumina. A ratio near unity implies equivalent activity per unit surface area. The relative rate of reaction for the Al particles was 10, with an estimated uncertainty of a factor of 2.

B. Pyridine Adsorption

We have also studied adsorption of the gaseous base, pyridine, with tunneling spectroscopy. Our crossed-film tunnel junctions (Al–oxide–Pb) were fabricated in a clean, high-vacuum evaporator. The general fabrication and testing procedure has been discussed elsewhere (*2*). Briefly, a thermally oxidized Al strip (0.2 mm wide, 1000 Å thick) on a glass slide was pretreated and doped with pyridine in a high-vacuum chamber as described below. Then five Pb cross-strips (0.2 mm wide, 3000 Å thick) were evaporated across the doped, oxidized Al strip. The completed junctions were tested with a low-power ohmmeter. Acceptable doped junctions had resistances in the range 50–1000 ohms. Electrical connections were made to acceptable junctions with small screw clamps. The junctions were immersed in liquid helium and tested to insure that all the current flow was due to electron tunneling. Finally, tunneling spectra, d^2V/dI^2 as a function of V, were plotted by applying an ac modulation current at a frequency of 1120 Hz and measuring the voltage at the second harmonic frequency with a lock-in amplifier.

At room temperature no pyridine adsorption was observed even with exposures of several Torr for tens of minutes. This does not mean that no pyridine adsorption occurred—only that none was adsorbed strongly enough to withstand evacuation and evaporation of the top metal electrode (*13*).

To increase the activity of the alumina we installed a 500 W tungsten–halogen lamp ≈10 cm away in the vacuum chamber to heat the oxidized Al strip. The lower

TABLE 1

Tunneling		Infrared				
Pyridine on alumina	Pyridine on florided alumina	Pyridine (*14*)	Pyridine complex with BH_3[a]	Other pyridine complexes (*14*)	Pyridinium ion (*15*)	Assignments (*16*)
	1637 w		1638 sh	1625–1650 w		
1605 sh		1602 mw				
1583 s	1612 s	1583 s[b]	1624 s	1597–1604 s	1638 ms	νC–C
1572 s	1573 s	1570 s	1580 mw	1568–1575 mw	1608 s	νC–C
	1547 w				1535 s	
1481 w	1490 mw	1478 m	1488 ms	1478–1489 m	1484 s	νC–C
1433 s	1447 s	1436 s	1459 s	1440–1449 s		νC–C
1372 w	1372 w	1372 w	1345 m	1370–1400 w		νC–C
1258 (broad)	1248 m		1250 m	1235–1242 w	1235 mw	
		1217 m		1215–1221 m	1194, 1326 m	δC–H
1153 m	1165 ms	1145 m	1170 s	1144–1168 m	1161 m	δC–H
1112 m					1030, 1050 m	
1064 m	1074 m	1067 m	1090 ms	1069–1082 ms		δC–H
1025 w		1031 ms	1060 m	1035–1042 ms		δC–C
975 m	1003 m	991 ms	1020 m	1005–1016 ms	1010 vw	νC–C
920 m	928 w	942 w	926 m	930–970 w[c]	980 mw	γC–H
860	880	886 w	885 vw		855 m	γC–H and Alumina
786 m						
740 m	760 m	747 s	756 s	750–769 s	738 s	γC–C
701 m	702 m	700 s	688–705 s	680–713 s	671 s	γC–H
615 m	650 ms	650 w		645–650 w[b]		δC–C
		601 s	604 vw	622–641 ms		δC–C
478 m	448 m					
404 s	390 s	403 m				γC–C

[a] See footnote 5 in the text.
[b] May be composite of resolvable bands at 1578 and 1593.
[c] Not visible in most complexes.

ctrae of Fig. 2 shows our results with a 60 sec preheat at 5×10^{-6} Torr and then 90 sec more heating with 1 Torr of pyridine. Table 1 compares the peak positions to those for pyridine (*14*), pyridine complexes (*14*),[5] and the pyridinium ion (*15*). Though the agreement is far from perfect, the peak positions most closely resemble those of unreacted pyridine. We conclude that the pyridine is only weakly adsorbed, not coordinately or ionically bonded. Clearly, more intense heating to remove surface hydroxyl groups from active sites would be desirable; the maximum sample temperature in our experiments was below 200°C.[6]

We have been able to generate Lewis acid sites even at these low temperatures with a liquid doping pretreatment. A 0.5 mg/ml solution of NH_4F in water was dropped onto the oxidized aluminum and the excess was spun off (*2*). The doped, oxidized aluminum was then returned to the vacuum chamber and heated and exposed to pyridine vapor as described above.

[5] Our own data on borane–pyridine complex from Aldrich Chemical Co. run neat between NaCl plates and in a AgCl cell.

[6] Perhaps the new strip heating technique developed by Bowser and Weinberg (**17**) will be useful for more intense heating.

The upper trace of Fig. 2 shows tunneling spectra for pyridine adsorption on this fluorided alumina. Examination of Table 1 shows that the agreement of peak positions is much better with pyridine complexes; the pyridine is coordinately bound to the alumina on Lewis acid sites. There are also weak peaks suggesting a small amount ionically bound to the alumina on Bronsted acid sites as observed by Hughes *et al.* (*18*) on fluorided alumina.

These results cannot be directly compared to results on standard aluminas because of different test conditions—in particular, less preheating. It is clear that at least fluorided, oxidized aluminum films exhibit Lewis acid properties attributed to γ-alumina and believed to be responsible for catalytic activity in some reactions (*19*). It also demonstrates that, as for standard aluminas, acidity is increased by fluoriding (*18*).

Finally, it is worth noting that at high temperatures (450–575°C), in oxygen, aluminum metal oxidizes thickly enough so that the resultant oxide layer can be directly analyzed by electron diffraction. The oxide layer is found to be γ-alumina (*20*).

CONCLUSION

In conclusion, the surface film of alumina formed on aluminum metal by oxidation in air is similar to standard γ-alumina in its properties. Thus, sensitive tunneling spectroscopy studies of adsorbed surface species on this alumina film (*4–6*) and on metals supported on this alumina will be relevant in investigating catalytic properties of aluminum surfaces.

REFERENCES

1. Jaklevic, R. C., and Lambe, J., *Phys. Rev. Lett.* **17**, 1139 (1966); Lambe, J., and Jaklevic, R. C., *Phys. Rev.* **165**, 821 (1968).
2. Hansma, P. K., *14th Int. Conf. Low Temp. Phys., Otaniemi, Finland, Proc.* **5**, 264 (1975); Hansma, P. K., *Phys. Rep.*, in press.
3. Langan, J. D., and Hansma, P. K., *Surface Sci.* **52**, 211 (1975).
4. Lewis, B. F., Mosesman, M., and Weinberg, W. H., *Surface Sci.* **41**, 142 (1974).
5. Lewis, B. F., Bowser, W. M., Horn, J. L., Jr., Luu, T., and Weinberg, W. H., *J. Vac. Sci. Technol.* **11**, 262 (1974).
6. Simonsen, M. G., Coleman, R. V., and Hansma, P. K., *J. Chem. Phys.* **61**, 3789 (1974).
7. Kimoto, K., Kamiya, Y., Nonoyama, M., and Uyeda, R., *Japan. J. Appl. Phys.* **2**, 702 (1963).
8. Hansma, P. K., Kaska, W. C., and Laine, R. M., *J. Amer. Chem. Soc.* **98**, 6064 (1976).
9. Selwood, P. W., private communication.
10. Peri, J. B., *J. Phys. Chem.* **69**, 211 (1965).
11. Bowser, W. M., and Weinberg, W. H., for publication.
12. Wefers, K., and Bell, G. M., "Oxides and Hydroxides of Aluminum" Alcoa Research Laboratories technical paper No. 19, 1972.
13. Kirtley, J., and Hansma, P. K., *Phys. Rev. B* **12**, 531 (1975).
14. Gill, N. S., Nuttal, R. H., Scaife, P. E., and Sharp, D. W. A., *J. Inorg. Nucl. Chem.* **18**, 79 (1961).
15. Cook, D., *Canad. J. Chem.* **39**, 2009 (1961).
16. Balaban, A. T., Mateescu, G. D., and Elian, M., *Tetrahedron* **18**, 1083 (1962).
17. Bowser, W. M., and Weinberg, W. H., *Rev. Sci. Instrum.* **47**, 583 (1976).
18. Hughes, T. R., White, H. M., and White, R. J., *J. Catal.* **13**, 58 (1969).
19. Parry, E. P., *J. Catal.* **2**, 371 (1963).
20. Beck, A. F., Heine, M. A., Caule, E. J., and Pryor, M. J., *Corrosion Sci.* **7**, 1 (1967).